

# Distribution Grid Topology Validation and Identification by Graph-based Load Profile Analysis

1<sup>st</sup> Mark Stefan

Center for Energy

AIT Austrian Institute of Technology GmbH AIT Austrian Institute of Technology GmbH

Vienna, Austria

mark.stefan@ait.ac.at

2<sup>nd</sup> Mario Faschang

Center for Energy

AIT Austrian Institute of Technology GmbH

Vienna, Austria

mario.faschang@ait.ac.at

3<sup>rd</sup> Stephan Cejka

Corporate Technology (CT)

Siemens AG

Vienna, Austria

stephan.cejka@siemens.com

4<sup>th</sup> Konrad Diwold

Corporate Technology (CT)

Siemens AG

Vienna, Austria

konrad.diwold@siemens.com

5<sup>th</sup> Alfred Einfalt

Corporate Technology (CT)

Siemens AG

Vienna, Austria

alfred.einfalt@siemens.com

6<sup>th</sup> Albin Frischenschlager

Corporate Technology (CT)

Siemens AG

Vienna, Austria

albin.frischenschlager@siemens.com

**Abstract**—Novel Smart Grid functions demand for reliable grid topology information. Currently, on distribution grid level, such information is only statically (i.e. configured once – e.g., in CIM or alike format) or not at all available. The static topology data may become invalid due to a switching action or grid extension. In this paper we present a Smart Grid application, which validates such a given CIM-represented grid topology on the basis of power profiles measured by grid monitoring devices. The topology is extracted as graph representation, field measurements are represented by an abstract grid model, and correlation of load profiles is calculated by a presented comparison algorithm. We demonstrate the application of the topology validation in the ASCR Smart City testbed and show its extension to a topology identification application. The two applications' field usage proves useful functions on which further Smart Grid applications will build upon.

**Index Terms**—Smart grids, Substation automation, Topology Identification, Pearson correlation

## I. INTRODUCTION

This section motivates our work, discusses the current state of grid topology research, and describes the environment in which we have developed the later presented topology validation and identification functions. Both functions are based on a comparison algorithm which is applied on several power profiles and their relations within a given topology, with the distinction that the validation algorithm checks if the current topology is valid whereas the identification tries to find a valid topology out of a set of potential topologies.

### A. Motivation

Power and voltage measurements from Low Voltage (LV) Grids without any knowledge about the dynamic topology or the respective distribution grid are of limited significance. Nevertheless, for basic applications (such as voltage control) it could be sufficient to work without topology information as only a defined voltage band must be maintained in the whole LV grid. If it is necessary to interact with distributed

actors to solve local voltage problems some kind of topology information is needed.

In case of urban LV grids, not voltage control but monitoring and controlling the loading of cables and transformers are the main tasks, in order to avoid overload situations. Therefore correct information about the current distribution grid topology is vital for such higher-level functions of modern automated distribution grids.

### B. Related Work and State of the Art

The open Common Information Model (CIM) standard [1], [2] is a widely used format for the representation of grid models and their topologies in productive environments (e.g., GIS, SCADA systems, power flow simulators). For applications on distribution grid level, necessary topology information is often unknown or the available topology information is not valid any longer due to undocumented topology changes or tripped circuit breakers. Different approaches exist to recover the correct topology information mostly based on the measurement of physical variables.

The author of reference [3] describes a methodology to recover grid topology from power flow between nodes represented as leafs and root nodes. This approach requires full knowledge of all power flow paths in the grid. In [4], an approach is presented to identify the grid topology with limited measurements, relying on voltage and angle measurements. Another approach to recover topology information is the formulation of an optimization problem, as described in [5]. Reference [6] developed a topology identification mechanism for power systems based on measured power injections at each bus. By using a learning algorithm they are able to infer the Laplacian matrix of a power system based on the measured power injections.

Another approach is the usage of a distribution grid's underlying communication infrastructure to infer on its topology. Such approaches are only viable if the communication

aligns with the grid topology, which can be the case when Power Line Communication (PLC) is used within a grid to communicate grid measurements. Accordingly a few studies have investigated how PLC properties can be used to infer a grid's topology (cf. [7], [8]).

In many applications graph theory is used to represent systems with components and connections between them. On one hand graphs can be used to illustrate a system (e.g., power grid), on the other hand the components and their interaction can be stored in matrices which might be used as input for calculations and analysis (cf. [9]–[12]).

### C. Environment

The application development and field operation environment bases on Gridlink – a communication middleware for intelligent secondary substations (iSSN), which we introduced in [13]. Gridlink-based systems are built of modules communicating with each other by exchanging messages. Several foundational applications, including a data storage module and the Grid Representation Module (GRM), constitute the "iSSN application frame" [14]. Most of these applications cannot run completely independent as they depend on input from other applications for their full functionality. Data originally approach the application frame via an IEC 60870-5-104 stack module, an information gateway to the field data concentrator allowing the integration of smart grid data into the applications [15]. A storage module respectively allows other applications to store and retrieve those data [13].

### D. Outline

In the following Section II we present the implementation of the topology validation (TOV) and topology identification (TID) feature, describing also the used data basis and the enforced algorithm. Subsequently, Section III contains the application of the TID and TOV features in the field – the Smart City testbed Seestadt Aspern in Vienna. We show the field setup, the topology graph representation, and the applications' interaction. Finally, we present the results based on processed field measurements and conclude the findings in Section IV.

## II. IMPLEMENTATION OF ISSN APPLICATIONS

This section gives an overview about the implementation of the applications running on intelligent secondary substations as well as information about used data and how to handle topology information.

### A. Data basis

The presented solution for distribution grid topology validation works on the basis of active power flow measurements between distribution grid nodes. The measurements are recorded from Grid Monitoring Devices (GMD) in the respective distribution grid testbed of Aspern Smart City Research (ASCR). Not all lines are fully monitored by these GMDs, thus we assume having one unmonitored feeder at each node where arbitrary power flow might occur. We work with

time series of three phase ( $A$ ,  $B$ , and  $C$ ) power measurements of  $n$  GMDs installed in the grid, stated in Equation 1.

$$\vec{P}_i = (P_{A,i}, P_{B,i}, P_{C,i})^T \quad \forall i \in [1..n] \quad (1)$$

Due to temporary unavailable communication links to the GMDs, the measured time series might have gaps lasting from some minutes to several hours. The typical sampling time is 150 seconds. Topology information is provided as XML-based *Common Information Model (CIM)* [1], [2], containing information about nodes, lines, transformers, connections, etc. This information is read by the GRM, the necessary data is extracted, and stored in representative data structures. For each device a unique numeric identifier is created. In general, an adjacency matrix is used in graph theory to store information about the connection between two elements (connected or not connected) but for our purposes, more information about the connections is needed. Therefore, we created some kind of extended adjacency matrix consisting of additional information (e.g., if the devices are directly or indirectly connected, the shortest path length between two devices, and if it is possible to reach an element when changing switch positions). Due to this extended connection information, the relation between two elements can be read very fast. The matrix is built initially when GRM is started and the topology information is fetched from the Storage Module. Based on the XML-based topology information and the representation as matrix, the topology can be illustrated as graph, consisting of nodes (representing devices) and lines (representing connections between the devices). An example will be presented in Section III, where results from field validation and identification are shown. Further information about the representation of the topology as matrix and graph can be found in previous publications (cf. [13] and [14]).

### B. Profile comparison algorithm

Due to the fact that we try to identify a relation between two GMDs, in particular check their parent-child-relation, we developed an algorithm to find the correlation between two time series. To choose a correct and reliable algorithm, we tested several approaches (e.g., outlier detection, frequency analysis). Some of them worked well for simulated data but not sufficient enough for field data. The best results – for simulated data as well as for field data – were achieved by applying Pearson Correlation for two power profiles, in particular using the sum of their phases. The correlation coefficient  $r_{\vec{P}_i \vec{P}_j}$  for profile  $\vec{P}_i$  and  $\vec{P}_j$  is calculated as stated in Equation 2 and will be within  $[-1; +1]$ .

$$r_{\vec{P}_i \vec{P}_j} = \frac{\sum_{k=1}^n (\vec{P}_{i_k} - \bar{P}_i)(\vec{P}_{j_k} - \bar{P}_j)}{\sqrt{\sum_{k=1}^n (\vec{P}_{i_k} - \bar{P}_i)^2} \sqrt{\sum_{k=1}^n (\vec{P}_{j_k} - \bar{P}_j)^2}} \quad (2)$$

where  $\vec{P}_i$  and  $\vec{P}_j$  are power profiles (series of measurement points, three phases aggregated),  $\bar{P}_i$  and  $\bar{P}_j$  are the mean values of series  $\vec{P}_i$  and  $\vec{P}_j$ , respectively.

As it is well-known from correlation functions, a high correlation coefficient indicates a high relation between the given data sets. For our developed algorithm, we defined a threshold to indicate whether a pair of GMDs can be interpreted as related or not. Based on several simulation runs and the field validation, a threshold value  $t = 0.75$  emerged as suitable for our purposes, resulting in

$$r_{\bar{P}_i \bar{P}_j} \begin{cases} < 0.75, & \text{No relations between profiles} \\ \geq 0.75, & \text{Relation between profiles} \end{cases}$$

As already mentioned in the previous section, there might be gaps within the time series due to connection losses, invalid data, or faulty sensors. Therefore, the data is analyzed before applying the comparison algorithm in a way that common timestamps between two profiles are identified and only these values are used for calculating the correlation.

Our profile comparison algorithm is used in several applications, in particular for topology validation, topology identification, and the assignment of measured buildings to measurement points within the grid. The following section will give an overview about the implementation of topology validation and identification, based on the presented comparison algorithm.

### C. Topology Validation and Identification

In many situations it might be necessary to validate the current grid topology. Assume a given topology with well-defined switch states and a set of measurement data within the grid. By applying the previously presented comparison algorithm on the set of profiles, a check can be executed whether the given topology is valid or – due to changes of switch states – not suitable for the current situation in the field any more. Based on the grid representation (Section II-A), the parent-child-relations under evaluation of all measurement points within the grid are available. Assuming a topology represented in Figure 1 with the relations in Equation 3 and 4.

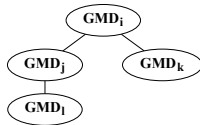


Fig. 1. Relation between four grid monitoring devices.

$$GMD_i \leftrightarrow GMD_j, GMD_k \quad (3)$$

$$GMD_j \leftrightarrow GMD_l \quad (4)$$

which indicates that  $GMD_j$  and  $GMD_k$  are child nodes<sup>1</sup> of  $GMD_i$ ;  $GMD_l$  is a child of  $GMD_j$ . Thus, the power profile of  $GMD_i$  contains at least the profiles of  $GMD_j$  and  $GMD_k$  but might contain more which are not measured or not available. As a result, Equation 5 and 6 should be valid.

$$GMD_j + GMD_k \subseteq GMD_i \quad (5)$$

$$GMD_l \subseteq GMD_j \quad (6)$$

<sup>1</sup> A child node is located in the topology *below* its parent node, which means it is closer to the consumer than its parent.

To validate the topology, the comparison algorithm is applied on the following pairs of power profiles (Equations 7 – 10).

$$GMD_i \leftrightarrow GMD_j \quad (7)$$

$$GMD_i \leftrightarrow GMD_k \quad (8)$$

$$GMD_i \leftrightarrow GMD_j + GMD_k \quad (9)$$

$$GMD_j \leftrightarrow GMD_l \quad (10)$$

Additionally to the validation of each pair of GMDs, the correlation is calculated for the aggregated power profile of all children (if there are more than one) and the GMD itself (stated in Equation 9). As a result, a correlation coefficient for each pair of profiles is calculated. If one of these values is less than the defined threshold  $t$ , the relation between the profiles cannot be confirmed and thus, the given topology is not valid. The overall result  $r$  of the topology validation is the minimum value of all correlation coefficients for all pairs  $(i, j)$  of power profiles which are under investigation, defined by  $r = \min(r_{\bar{P}_i \bar{P}_j})$ . As a result, the execution time of the algorithm can be stated as  $\mathcal{O}(n^2)$  where  $n$  indicates the number of GMDs.

An expansion state of the topology validation is the topology identification: If a set of topologies (i.e. a set of CIM topology information) is available and it is not clear which one is the actual used topology, the validation is executed on each topology resulting in one of the following cases: i) None of the topologies match with the power profiles, more precisely the overall correlation coefficient  $r_x$  for each topology  $x$  is less than the threshold  $t$ . Thus, none of the topologies is valid. ii) The correlation coefficient  $r_x$  is valid for exactly one topology  $x$  and therefore, this topology can be interpreted as currently used. iii) For more than one topology the correlation coefficient is at least as high as the threshold and thus, a valid topology. Then, the topology with the highest correlation coefficient is used as the current one.

To sum up, the topology identification is based on the topology validation but executed on a set of topologies. The best validation result will determine the topology corresponding to the used power profiles. This approach can be used for analyzing the current grid situation, but also for investigations on previous grid states. In some cases the validation and identification of the topology should be treated with caution, for example when using short profile length or profiles with non-significant behavior. The following section will present the application of the validation and identification algorithm in the field and show results for valid and invalid topologies as well as the comparison when using different lengths of power profiles and the effect on the results of the profile comparison algorithm.

### III. APPLICATION IN THE FIELD

After the previously presented implementation details for the topology validation and topology identification modules, follows hereafter a detailed field application example. Furthermore, the limitations of the algorithms are discussed and

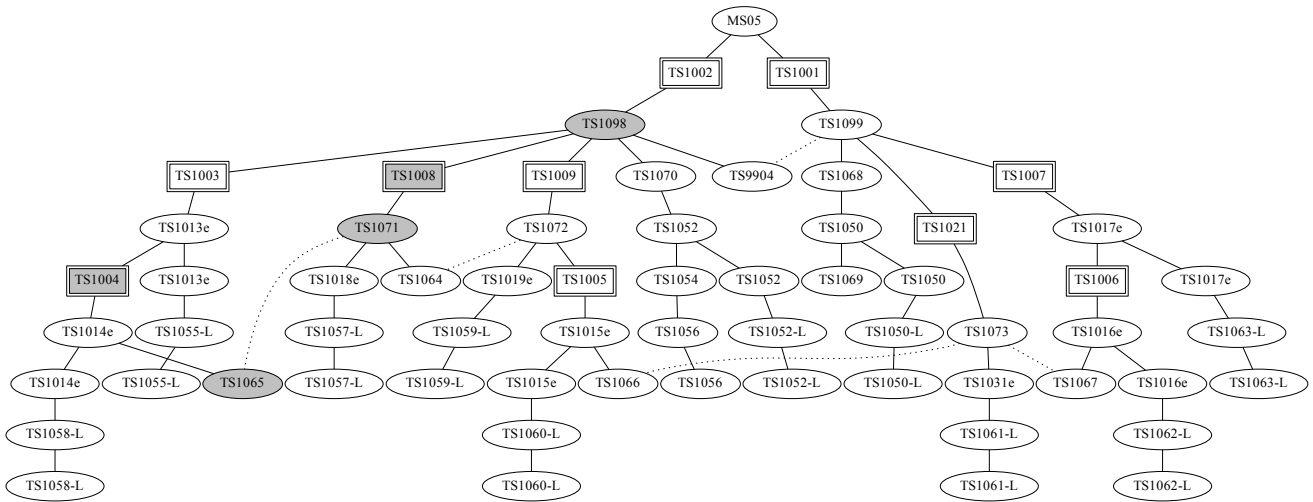


Fig. 2. Grid topology graph used for validation and identification. Rectangular nodes represent the grid monitoring devices, round nodes all other devices within the topology. The connections between gray nodes differ in the used valid and invalid topology (TS1098-TS1008, TS1071-TS1065). Solid lines between nodes represent closed connections whereas dotted lines represent open connections.

a performance analysis is presented. Additional information concerning the hardware set-up in the field and the interaction between the modules can be found in [14].

#### A. Topology Validation and Topology Identification in the field

Topology information is provided from the SCADA system. The corresponding CIM files as well as the GMD measurements are stored in the local storage module. The topology to be evaluated – from Aspern Smart City Research (ASCR); within the research project *Smart City Demo Aspern* [16] – is shown in Figure 2 as graph representation. It contains a substation node at the top (*MS05*), several consumers (indicated by suffix *-L* in the node name), and other components (e.g., lines, switches). Components which contain Grid Monitoring Devices (GMD) are shown as rectangular nodes, all others are circles. The solid lines between nodes indicate that these nodes are directly connected and potentially existing switches are closed whereas dotted lines represent open switches. Corresponding power profiles are stored in the Storage Module and sent to TOV via the GRM. For our field validation, time series starting at 2017/01/02 until 2017/01/11 are used. Power values  $\vec{P}_i$  (in kW) of all grid monitoring devices within this period of time are shown in Figure 3 in the first five plots, grouped by their parent-child-relationship. For example, the first plot shows the GMD *TS1002* with its child-GMDs *TS1003*, *TS1008*, and *TS1009* as well as the aggregation of its child profiles *TS1003+TS1008+TS1009*.

When using the comparison algorithm, the results will vary, depending on the length of the profiles. If very short profiles are used, the output of the algorithm might result in *false positives* (matching between two profiles found although there is no physical dependency) or *false negatives* (no matching found due to an uncertain behavior of the consumers within the chosen period, cf. [17]). To find a suitable profile length where the presented algorithm produces reliable results,

several lengths were investigated (six hours, twelve hours, one day, one week). The topology identification was started every six hours, using the valid topology from Figure 2 on one hand and an invalid one (connection between *TS1098* and *TS1008* opened, connection *TS1065* and *TS1071* closed; therefore *TS1008* would be a child node of *TS1004*, illustrated by filled gray nodes in the Figure 2) on the other hand.

Results for the correlation coefficient  $r$  at every six hours for different profile lengths using the invalid topology are depicted in the second last plot and for the valid topology in the last plot of Figure 3. Additionally, the threshold value for  $r$  (0.75) is drawn as dotted line in both plots. The correlation coefficient  $r$  for a valid topology should be at least as high as the threshold line whereas the results for the invalid topology should be below the threshold. In both cases the variation of the results for profiles with a length of six hours, twelve hours, and one day is very high and jump above and below the threshold – the shorter the profile length, the higher this effect. In comparison to these observations, a profile length of one week results in slightly varying results, shown as thick line in both plots, which is constantly below the threshold for the invalid topology and above for the valid one. On the other hand, a very long profile might result in a validated topology although a switch state change occurred within this period and long data sets needed for the comparison causing higher network traffic, delays, and execution time. Figure 4 shows the power profiles of two GMDs. Node *TS1021* is the parent-node of *TS1061-L*. Obviously, at the child-node, some generation happens at that period of time, indicated by the green line reaching negative values. The application of the topology validation for these exemplary power profiles results in a correlation value of  $r = 0.98$  due to the very similar behavior of the two measurements. Summing up, the validation algorithm as well as the topology identification show the expected results and are ready to be used in live operation.

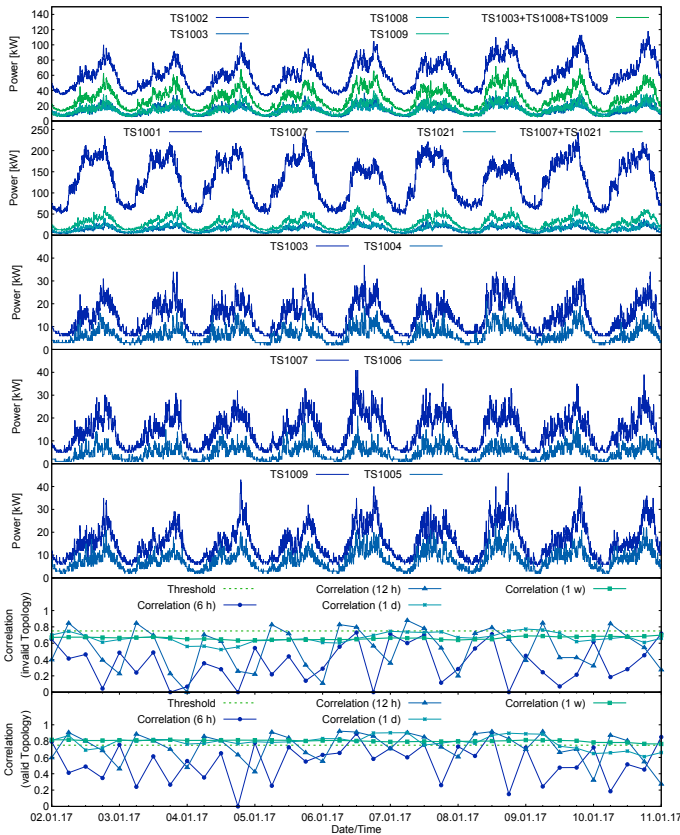


Fig. 3. Power profiles and correlation results for different profile lengths, valid and invalid topologies. The first five plots show the power profiles between 2017/01/02 and 2017/01/11, grouped by their parent-child-relation. The last two plots show the results of the topology validation for an invalid and a valid topology.

Attention must be paid to the length of the profiles used for comparison algorithm and the threshold. Due to the fact that active generation at nodes also influences the behavior of their parent-nodes, the algorithm can handle both, consumption as well as generation.

### B. Limitations and extensions of the method

In general, the higher the number of measurement devices within the monitored distribution grid, the higher is the reliability of the correlation result: If all child-nodes of a particular measured node are monitored, the aggregated child-profiles will be very similar to the profile of the parent-node, deducting inaccuracies in measurements and timing delays. Thus, in complete monitored grids, it is sufficient to apply the comparison algorithm only to a node and its aggregated child nodes, the comparison of single child nodes with their parent nodes can be renounced. On the other hand, unmonitored devices will have a negative effect on the overall comparison result which emerged in the previously presented example by comparing profiles *TS1021* and *TS1007* with their parent node *TS1001* where a high amount of power was not monitored on a third branch, starting at node *TS1068* (second plot in Figure 3). In case of faulty measurement devices for a longer period

of time the same problem as mentioned above arises: The comparison algorithm can only be applied on the remaining devices. For short temporary outages of single GMDs, only overlapping parts of the profiles are used for the comparison and may have only negligible effects on the results. Bad measurement data (e.g., outlier or distortions like abnormally high or low values) will have no significant effect on the correlation result if the occurrence is within a short period of time. Nevertheless, handling of faulty measurement values is not part of the algorithm and should be done before the correlation results are calculated. The previously presented algorithm is applied on aggregated power profiles due to the circumstances of the topology and the measured power profiles. Another option would be the application on each single phase of the monitoring devices which might be feasible in other power grids, especially if there is a high number of single-phase end users. To calculate the overall result of the comparison algorithm several approaches might be used: Average result of all phases, highest correlation value of all phases is considered, lowest correlation values of all phases is considered. Another possibility for applying this type of comparison algorithm would be the usage of other physical values (e.g., voltage or current) instead of power measurements. Another limitation of the presented method is the detection of switch state changes. If such a change occurred within the used profile, the result of the correlation can be valid or invalid, depending on the impact on the parent-nodes and the temporal position within the considered profile. In summary, it can be stated that the reliability of the results depends on several factors, whereas the best results are achieved if all branches and sub-branches of the topology are monitored and significant power profiles are measured. In such situations, short profile lengths are sufficient to obtain adequate results. Otherwise, a feasible trade-off between the used profile-length with respect to undetected changes of switch state and too short profiles must be found. Introducing a method to detect significant parts of the profiles could further increase the quality of the results.

### C. Performance of the algorithm

Table I shows the runtime of the topology validation on a Windows 7 desktop PC<sup>2</sup> and on the used industry-grade PC<sup>3</sup> in the field with ten power profiles and ten executions of the comparison algorithm. In a distribution grid with  $n$  switches,  $2^n$  possible switch positions are available and therefore, theoretically also  $2^n$  different topologies. Due to the fact that several topologies are not useful (e.g., due to non-supplied nodes) and others are avoided in the field (e.g., closed circles) or preferred, an operable number of different topologies is taken into account for the topology identification. Additionally, the algorithm is applied on the substation level and therefore, only a manageable number of nodes with measured power profiles are available. As a consequence, the presented approach for validating or identifying a topology

<sup>2</sup>Intel Core i7-4600 CPU, 2.10 GHz, 8 GB RAM, Windows 7 (64 Bit)

<sup>3</sup>Intel Atom CPU, 1.3 GHz, 2 GB RAM, Debian Linux (32 Bit)

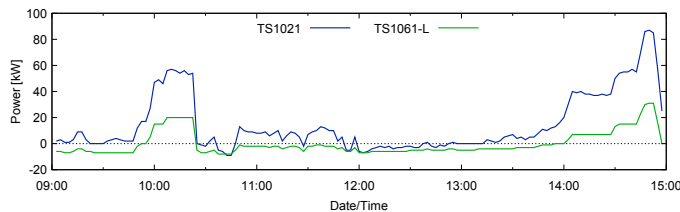


Fig. 4. Aggregated active power profile for a parent-node (*TS1021*) and a child-node (*TS1061-L*) with PV generation.

is a feasible solution for the requirements in the domain of distribution grids where results of these procedures are expected within several seconds up to minutes.

TABLE I

COMPARISON OF ALGORITHM RUNTIME FOR THE PRESENTED EXAMPLE.

Profile length	Runtime [ms] (desktop PC)	Runtime [ms] (ind.-grade PC)
6 hours	170	260
12 hours	260	400
1 day	300	500
1 week	440	2.500

#### IV. CONCLUSION

The presented TOV and TID modules have successfully been embedded into the “iSSN application frame” [14] and have been field-tested in the Smart Grid testbed of the ASCR, operating in the Seestadt Aspern (Vienna) – currently one of Europe’s biggest urban development projects. Static distribution grid topology (provided as CIM data stream) is read by the Grid Representation Module and stored within a matrix, graph-based representing devices and their links. The Storage Module provides field-measured power profiles. These profiles are used to validate or identify the current topology, respectively. Several algorithms for comparing power profiles have been tested – most of them worked well with simulation data but only the Pearson Correlation-based comparison algorithm was feasible for field applications. As a consequence, it is implemented in the topology validation as well as for the identification of the currently used topology. Both applications have been applied in the field and tested with real measurements. The analysis of the results showed that the applications performed well and created the expected outputs for topology identification and validation. The field trial also showed that the length of the profiles is an important factor regarding the quality of the validation algorithm. Short profiles may lead to false positive or false negative results, respectively. Thus, a profile length of one week seemed feasible in order to avoid impact of temporary profile deviations on the validation results. Within very long profiles, switch position changes might be overlooked. A comparison of different profile lengths was given and evaluated in the field and due to the results, the deployment of the applications in real operation is possible.

#### ACKNOWLEDGMENT

The presented work is developed in the Smart Grid testbed of Aspern Smart City Research and conducted in the research projects *SCDA – Smart City Demo Aspern* (846141), funded within the program *Smart Cities* by the Austrian *Climate and Energy Fund* and *iNIS – Integrated Network Information System* (849902), funded within the program *ICT of the Future* by the Austrian Federal Ministry for Transport, Innovation and Technology (*bmvit*).

#### REFERENCES

- [1] “IEC 61970: Energy management system application program interface (EMS-API) - Part 301: Common information model (CIM) base, Third Edition,” Tech. Rep., 2009.
- [2] M. Usler *et al.*, *The Common Information Model CIM: IEC 61968/61970 and 62325 - A practical introduction to the CIM*. Springer Science & Business Media, 2012.
- [3] C. Benoit, “Models for investigation of flexibility benefits in unbalanced low voltage smart grids,” Thesis, Université Grenoble Alpes, Jun. 2015. [Online]. Available: <https://tel.archives-ouvertes.fr/tel-01223369>
- [4] Y. Sharon, A. M. Annaswamy, A. L. Motto, and A. Chakraborty, “Topology identification in distribution network with limited measurements,” in *2012 IEEE PES Innovative Smart Grid Technologies (ISGT)*, Jan 2012, pp. 1–6.
- [5] L. Zhao, W. Z. Song, L. Tong, Y. Wu, and J. Yang, “Topology identification in smart grid with limited measurements via convex optimization,” in *2014 IEEE Innovative Smart Grid Technologies - Asia (ISGT ASIA)*, May 2014, pp. 803–808.
- [6] X. Li, H. V. Poor, and A. Scaglione, “Blind topology identification for power systems,” in *Smart Grid Communications (SmartGridComm), 2013 IEEE International Conference on*. IEEE, 2013, pp. 91–96.
- [7] M. O. Ahmed and L. Lampe, “Power line communications for low-voltage power grid tomography,” *IEEE Transactions on Communications*, vol. 61, no. 12, pp. 5163–5175, 2013.
- [8] T. Erseghe, S. Tomasin, and A. Vigato, “Topology estimation for smart micro grids via powerline communications,” *IEEE Transactions on Signal Processing*, vol. 61, no. 13, pp. 3368–3377, 2013.
- [9] K. Sun, “Complex networks theory: A new method of research in power grid,” in *2005 IEEE/PES Transmission Distribution Conference Exposition: Asia and Pacific*, 2005, pp. 1–6.
- [10] P. Hines, S. Blumsack, E. C. Sanchez, and C. Barrows, “The topological and electrical structure of power grids,” in *2010 43rd Hawaii International Conference on System Sciences*, Jan 2010, pp. 1–10.
- [11] E. Jenelius, “Graph Models of Infrastructures and the Robustness of Power Grids,” Master’s thesis, Royal Institute of Technology (KTH), Stockholm, Sweden, 2004.
- [12] D. Deka, S. Backhaus, and M. Chertkov, “Structure learning in power distribution networks,” *arXiv preprint arXiv: 1501.04131*, 2015.
- [13] M. Faschang, S. Cejka, M. Stefan, A. Frischenschlager, A. Einfalt, K. Diwold, F. Prösl Andrén, T. Strasser, and F. Kupzog, “Provisioning, deployment, and operation of smart grid applications on substation level,” *Computer Science - Research and Development*, vol. 32, no. 1, pp. 117–130, 2017.
- [14] M. Faschang, M. Stefan, F. Kupzog, A. Einfalt, and S. Cejka, “‘iSSN Application Frame’ – a flexible and performant framework hosting smart grid applications,” in *CIREC Workshop 2016*, Jun 2016, paper 255.
- [15] A. Einfalt, S. Cejka, K. Diwold, A. Frischenschlager, M. Faschang, M. Stefan, and F. Kupzog, “Interaction of smart grid applications supporting plug & automate for intelligent secondary substations,” *CIREC, Open Access Proceedings Journal*, vol. 2017, no. 1, pp. 1257–1260, Oct 2017.
- [16] Aspern Smart City Research GmbH & Co KG (ASCR), “SCDA – Smart City Demo Aspern,” <http://www.ascr.at/foerderungen/scda/>, 2016, [Online; accessed 24-05-2017].
- [17] P. Zehetbauer, S. Kloibhofer, M. Stifter, B.-V. Mysore-Vasudevarao, and F. Leimgruber, “Identification and reconstruction of photovoltaic measurement gaps based on temporal correlation and spatial distance,” in *6th International Workshop in Integration of Solar Power into Power Systems (SIW 2016)*, 2016, pp. 276–282.